Shrinking and splitting of drainage basins in orogenic landscapes from the migration of the main drainage divide — Source link ↗

Stéphane Bonnet, Stéphane Bonnet

Institutions: University of Rennes, Centre national de la recherche scientifique

Related papers:

- Dynamic reorganization of river basins.

- Dynamics of the stream-power river incision model: Implications for height limits of mountain ranges, landscape response timescales, and research needs

- Orogeny and orography: The effects of erosion on the structure of mountain belts

- Landscape response to climate change: Insights from experimental modeling and implications for tectonic versus climatic uplift of topography

- Coupled numerical–analytical approach to landscape evolution modeling

Shrinking and Splitting of drainage basins in orogenic landscapes from the migration of the main drainage divide

Stéphane Bonnet

Shrinking and Splitting of drainage basins in orogenic landscapes from the migration of the main drainage divide

STEPHANE BONNET [1,2]

[1]Géosciences Rennes, Université de Rennes 1, Campus de Beaulieu, 35042 Rennes Cedex, France

[2]CNRS/INSU, UMR 6118, Campus de Beaulieu, 35042 Rennes Cedex, France

e-mail: stephane.bonnet@univ-rennes1.fr

Phone +33 2 23 23 56 90

Fax +33 2 23 23 67 80

Climate, and in particular the spatial pattern of precipitation, is thought to affect the topographic and tectonic evolution of mountain belts through erosion[1–5]. Numerical model simulations of landscape erosion controlled by horizontal tectonic motion[6] or orographic precipitation[7,8] result in the asymmetric topography that characterizes most natural mountain belts6, and in a continuous migration of the main drainage divide. The effects of such a migration have, however, been challenging to observe in natural settings6. Here I document the effects of a lateral precipitation gradient on a landscape undergoing constant uplift in a laboratory modelling experiment. In the experiment, the drainage divide migrates towards the drier, leeward side of the mountain range, causing the drainage basins on the leeward side to shrink and split into smaller basins. This mechanism results in a progressively increasing number of drainage basins on the leeward side of the mountain range as the divide migrates, such that the expected relationship between the spacing of drainage basins and the location of the main drainage divide[9] is maintained. I propose that this mechanism could clarify the drainage divide migration and topographic asymmetry found in active orogenic mountain ranges, as exemplified by the Aconquija Range of Argentina[10].

   In separating the water flux coming from precipitation between the drainage basins located over the two opposite flanks of topography, the main drainage divide is an important physiographic element of orogen topography. When associated with an orographic effect, drainage divide delineates domains where differences in precipitation and hydrologic regimes may directly influence erosional processes that shape topography and thus, landscape forms[7,8], erosion rates[11] and, over a geological time-scale, the rates and patterns of exhumation of metamorphic rocks[4] and internal strain[3] within the orogens. The continuous migration of the drainage divide in orogens, as observed in the numerical modelling of surface processes when erosion is forced by tectonic advection[6] or orographic precipitations[7,8], is hardly demonstrable in natural settings. Only the observation that natural orogens usually exhibit asymmetric topography[6] supports numerical results. In natural settings, divide dynamics have only been inferred in local and timely-discontinuous shifts in their location consecutive to river capture events[12]. They have also occasionally been inferred from changes in sediment content at the drainage basin outlets[13]. This emphasizes the need to find criteria that can be used to better investigate divide migration in orogens.

40   The experimental modelling of erosion is a powerful tool to investigate landscape dynamics.
41   It indicates that landscapes may be more dynamic than the numerical models suggest[14], e.g. when
42   considering the evolution of ridge crests, and it has already been used to demonstrate that some
43   landscape features, such as long narrow perched drainages, form in areas of actively migrating
44   divides[15]. Figure 1 shows an example of divide migration in the laboratory modelling of landscape
45   dynamics[16,17] forced by uniform uplifting of the eroded material but with a precipitation gradient (see
46   the Methods section). In this experiment, the precipitation gradient was applied after a first phase of
47   uniform precipitation and the attainment of a steady state between erosion and uplift[16,17] (Fig. 1).
48   During this initial phase, the topography is symmetric overall (Fig. 1a, Fig. 1c), and the elevation of
49   the divide remains constant with time (Fig. 1a, Fig. 1b). Application of the precipitation gradient
50   induces migration of the drainage divide toward the drier side of the landscape and development of
51   an asymmetric topography (Fig. 1), as also observed numerically[7,8]. The divide is simultaneously
52   uplifted (Fig. 1b) such that the mean topographic slope of the wetter side of the landscape remains
53   constant during its elongation (Fig. 1a). At no time is the establishment of a new steady-state
54   observed in this experiment (Fig. 1b), nor is the divide position pinned (Fig. 1c). The progressive
55   shortening of the drier side of the landscape consecutive to divide migration results in an increase in
56   the roughness of the surface and in a very unstable landscape (Fig. 2).This leads to an original
57   mechanism that splits the drainage networks: each initial drainage network splits into two individual
58   networks that become progressively separated by the growth of a new hillcrest (Figure 2). Through
59   this mechanism, the numbers of drainage basins extending to the main divide increases during divide
60   migration.

61   Given the pattern of rainfall and once the precipitation gradient is applied, the migration of
62   the drainage divide induces a continuous decrease in the mean runoff within the drainage basins
63   located on the drier side of the landscape (Fig. 3b). There, the area of the drainage basins decreases
64   because of the combination of two processes: a continuous size reduction (a direct consequence of
65   the divide migration), and an abrupt size reduction consecutive to the split of the drainage network
66   and the individuation of two drainage basins from a previous single one. Overall, the decrease of the
67   drainage basins' size correlates with a steepening of their channels (Fig. 3c). The detailed analysis of
68   the experimental drainage basins' response to the rainfall gradient documents a two-step evolution
69   of the channels, before and after splitting occurred (Fig. 3). In a first phase, from the establishment of
70   the precipitation gradient up to the splitting, an erosion wave propagates upward within the former
71   steady-state channels (Fig. 3c). It generates the upstream migration of a knickpoint, defined as an
72   abrupt change in the channel gradient, which separates an upstream segment passively uplifted from
73   a downstream segment steepened to a new steady-state gradient (Fig. 3c). This mechanism has
74   already been described analytically[18,19] and experimentally[16]. After the erosion wave has swept the
75   entire channels, channel steepening drives a temporary steady-state between uplift and erosion (Fig.
76   3 c,d). This temporary steady-state only concerns channels and not the whole landscape (Fig. 1), as
77   hillcrests are passively uplifted at the same time (Fig. 3d). In a second phase, after the split of
78   drainage networks, a profound disruption of the temporary steady-state of the channels occurs,
79   preventing the establishment of new steady-state conditions. From splitting onward, the channels
80   continuously steepen as they shorten because of divide migration (Fig. 3c). Figure 3d shows the
81   elevation history of three geographically-fixed spatial points of the model, illustrating how complex
82   elevation histories can be during this sequence of landscape changes. Specifically, it illustrates how

83   some parts of the floodplains are uplifted and transformed into a divide separating the two newly-
84   formed drainage basins after splitting has occurred.

85   As for natural channels[20], the hydraulic properties, width, depth, cross-sectional area, mean
86   flow velocity, hydraulic radius and wet perimeter all increase with water discharge in the
87   laboratory[21]. By continually reducing the discharge within drainage basins, divide migration
88   consequently drives a narrowing of the channels so that erosion is progressively localized within the
89   floodplains during divide migration, resulting in their abandoned parts being uplifted (Fig. 3d).
90   Channels have also been shown to narrow as they steepen, theoretically[22] and in the field[23], so that
91   narrowing may also be driven by the steepening of the channels described here (Fig. 3c). Even if
92   channels cannot be observed directly during experiments because of opacity during rainfall, a careful
93   examination at the time-step evolution of the experimental landscape (Fig. 2) shows that the location
94   of the newly-formed trunk channels after splitting is intimately linked to the former geometry of the
95   upstream tributaries of the channel network. As illustrated in Figure 4, the network splitting
96   mechanism most likely occurs at the tributaries' junction and lies in the combination of channel
97   narrowing associated with ongoing uplift and reduced erosion rates in the interfluves area (Fig 3d).
98   This enables flows coming from the tributaries to disconnect in place of a former single channel.
99
100   The mechanism of network splitting proposed here led to transient dynamics that are
101   exemplified by the Sierra Aconquija range in the Sierras Pampeanas province of NW Argentina[10] (Fig.
102   5). The Aconquija is an uplifted basement range, bounded by active high-angle reverse faults on one
103   or both sides against Neogene sedimentary basins[10,24-25] (Fig. 5). Thermochronological data[10]
104   indicates the start of the rapid exhumation of the range ~6 Ma ago and a total rock uplift of at least
105   6.4-11.1 km over the last 6 Myr. It presently forms a prominent landscape above its adjacent
106   foreland plains, reaching elevations > 5 km. Because of its location on the eastern front of the Andes,
107   representing a major topographic barrier to the moisture flux coming from the Atlantic Ocean[26], the
108   Sierra Aconquija is an orographic barrier: its eastern flank receives much more precipitation (> 2 m
109   yr^{-1}) than its western one[10,25-26] (Fig. 5), where an arid climate prevails. To the west of the Aconquija,
110   climate proxies indicate that aridification initiated 3 Myr ago[27]. It is interpreted as reflecting the
111   onset of the orographic barrier via a surface uplift of the Aconquija[27], which occurred when the
112   topography reached elevations of 2-2.5 km in the Andes[10]. Compared to modern maximum
113   elevations of the range, this suggests that the divide of the Aconquija has been uplifted (surface
114   uplift) by 3-3.5 km during the last 3 Myr[10]. The Aconquija presently shows a jagged topography
115   characterized by deeply-incised, regularly-spaced, transverse rivers. Overall, its topography is
116   asymmetric and its drainage divide shows an offset position toward the drier side of the range (Fig.
117   5), with a fractional divide position[6] of 0.6-0.7. The drainage networks on the drier leeward flank of
118   the range show multiple examples of unusual landscape configurations (Fig. 5c), indicating that the
119   split of drainage networks likely occurred following the mechanism described experimentally (Fig. 4).
120   It implies the migration of the main divide of the Aconquija toward the drier flank of the range and
121   the progressive development of its topographic asymmetry. The asymmetric development of
122   topography would not exist in the absence of asymmetry of at least one forcing parameter[6]: rock
123   erodability, tectonic forcing or climatic conditions. Differences in erodability are not likely to be the
124   cause of the asymmetry because variations in topography do not coincide with lithologic ones.
125   Horizontal tectonic motions are likely negligible in the Aconquija case because of the high-angle of

126   the bounding faults[10,24] and because the range is bounded by opposite reverse faults on both sides in

127   the area considered (Fig. 5). The development of the topographic asymmetry of the Aconquija is

128   most likely the direct result of climate, through the establishment of the orographic rainfall gradient,

129   following a mechanism of orographic influence on asymmetry development also observed

130   numerically[7,8]. Indirectly[28], climatic variations led to different sequences of aggradation and

131   degradation events in sedimentary basins flanking the range and resulted in a base-level more

132   elevated on the leeward side than on the windward one[10], a phenomenon that may also have

133   influenced topographic asymmetry development. Assuming a symmetric topography at the onset of

134   orographic barrier development 3 Myr ago[27], the subsequent estimated rate of divide migration is

135   ~0.8-1.5 mm yr^{-1}, of the same order of magnitude as uplift rates.

136   In natural settings, the spacing of drainage basin outlets along mountain fronts is remarkably

137   regular, regardless of their tectonic and climatic settings[9,29]. With the exception of some Himalayan

138   catchments[9], most landscapes obey a single empirical scaling law, which relates outlet spacing to half

139   the distance between the main divide and the range front[9,29]. As studied here, the experimental

140   landscapes follow a similar law (see Supplementary Figure). In the context of widening mountain

141   belts, the preservation of the spacing ratio implies that processes such as river capture or drainage

142   divide collapse decrease the number of outlets during the lengthening of drainage basins[9,29]. The

143   present study demonstrates that the reverse occurs during the shortening of drainage basins induced

144   by divide migration, and the split of drainage networks described here represents the only existing

145   mechanism that allows to increase the number of drainage basins at mountain fronts and to

146   maintain their spacing ratio. Experiments illustrate how complex the elevation history of a spatial

147   point of a landscape can be. Many issues must still be investigated to better understand the

148   mechanism of drainage splitting, both in experiments and nature; the channel behaviour at the

149   tributaries' junction in the context of reducing discharge is likely the most important. However, the

150   identification of the splitting mechanism provides the first opportunity to investigate drainage divide

151   migration in active orogens through the coeval dynamics of the associated drainage networks.

152

153   **METHODS**

154   Experiments were performed in the Modelling Laboratory at Geosciences Rennes/University

155   of Rennes1. I used a paste of pure silica grains (mean grain size of 20 μm) mixed with water. The

156   water content was chosen such that the paste has a vertical angle of rest and water infiltration was

157   negligible. The paste was introduced into a box with a vertically adjustable base, whose movements

158   were driven by a screw and a computer-controlled stepping motor. The internal area of the box was

159   60 X 40 cm and 50 cm deep. During an experimental run, the base of the box was raised at a constant

160   rate and pushed the paste outside the top of the box at a rate defined as the uplift rate. Precipitation

161   was generated by a system of four sprinklers that delivered water droplets with diameter of ~10 μm,

162   which was small enough to avoid any splash dispersion at the surface of the model. The precipitation

163   rate at the surface of the model could be controlled by changing the water pressure and the

164   configuration of the sprinklers. Precipitation was measured by collecting water in 20 pans at the

165   location of the model before and after each experimental run. The coefficient of variation (standard

166   deviation/mean) of rainfall rates for measurement intervals of 10 minutes is less than 5 % for the

167 experiment performed here. The surface of the model was eroded by running water at its surface
168 and grain detachment and transport occurred mainly by shear detachment through surface runoff.
169 The topography was measured by using a commercial stereogrammetric camera system, which has a
170 precision of ~20 µm. The raw data were gridded to produce DEMs with a pixel size of 0.5 mm.

171   Inherently to all laboratory modellings of landscape dynamics (at University of Rennes 1: see
172 refs. 16, 17, 21 and at University of Minnesota: see ref. 14 and 15), experiments such as those
173 developed here are oversimplifications of natural systems. Oversimplification is imposed by the
174 difficulty to model some particular processes (vegetation dynamics, weathering processes and
175 chemical erosion, atmospheric processes, etc.) but it is also a choice that is motivated by the
176 necessity to understand the influence of each forcing parameter before investigating more complex
177 systems. More importantly, experiments cannot be scaled to nature because of the impossibility to
178 downscale natural conditions to the laboratory (for examples, see refs. 15, 17, 21). Because of these
179 scale distortions, modelling of landscape dynamics is only experimental and not analog[15-17]. However,
180 there is a consensus about the qualitative relevance of these models[15-17], which permits a much more
181 dynamic view of landscape evolution than the usual numerical models (see ref. 15).

182

183 **References**

184 1. Beaumont, C., Fullsack, P. & Hamilton, J. Erosional control of active compressional orogens.
185   In *Thrust Tectonics* (ed McClay, K. R.) 1-18 (New York: Chapman Hall, 1992)
186 2. Hoffman, P. F. & Grotzinger, J. P. Orographic precipitation, erosional unloading, and tectonic
187   style. *Geology* **21,** 195-198 (1993).
188 3. Willett, S. D. Orogeny and orography: The effects of erosion on the structure of mountain
189   belts. *J. Geophys. Res* **104,** 28957-28981 (1999).
190 4. Montgomery, D. R., Balco G. & Willett, S. D. Climate, tectonics, and the morphology of the
191   Andes. *Geology* **29,** 579-582 (2001).
192 5. Whipple, K. X. The influence of climate on the tectonic evolution of mountain belts. *Nature
193   Geosci.* **2,** 97-104 (2009).
194 6. Willett, S. D., Slingerland, R. & Hovius, N. Uplift, shortening, and steady-state in active
195   mountain belts. *Am. J. Sci.* **301,** 455-485 (2001).
196 7. Roe, G. H., Montgomery, D. R. & Hallet, B. Orographic precipitation and the relief of
197   mountain ranges. *J. Geophy. Res.* **108** (2003) (doi:10.1029/2001JB001521).
198 8. Anders, A. M., Roe, G. H., Montgomery, D. R. & Hallet, B. Influence of precipitation phase on
199   the form of mountain ranges. *Geology* **36,** 479-482 (2008).
200 9. Hovius, N. Regular spacing of drainage outlets from linear mountain belts. *Basin Res*. **8,** 29-44
201   (1996).
202 10. Sobel, E. R. & Strecker, M. R. Uplift, exhumation and precipitation: Tectonic and climatic
203   control of late Cenozoic landscape evolution in the northern Sierras Pampeanas, Argentina.
204   *Basin Res.* **15,** 431-451 (2003).
205 11. Reiners, P. W., Ehlers, T. A., Mitchell, S. G. & Montgomery, D. R. Coupled spatial variations in
206   precipitation and long-term erosion rates across the Washington Cascades. *Nature* **426,** 645-
207   647 (2003).

208 12. Craw, D., Nelson, E. & Koons, P. O. Structure and topographic evolution of the Main Divide in
209   the Landsborough-Hopkins area of the Southern Alps, New Zealand. *New Zealand J. Geol.*
210   *Geophys.* **46,** 553-562 (2003).
211 13. Kuhlemann, J., Frisch, W., Dunkl, I., Székely, D. & Spiegel C. Miocene shifts of the drainage
212   divide in the Alps and their foreland basin. *Z. Geomorph. N. F.* **45,** 239-265 (2001).
213 14. Hasbargen, L. E. & Paola, C. Landscape instability in an experimental drainage basin. *Geology*
214   **28,** 1067-1070 (2000).
215 15. Hasbargen, L. E. Some Characteristics of Drainage Basin Realignment. Eos Trans. AGU, 87(36),
216   Jt. Assem. Suppl., Abstract H53F-04 (2006).
217 16. Bonnet, S. & Crave, A. Landscape response to climate change: Insights from experimental
218   modeling and implications for tectonic versus climatic uplift of topography. *Geology* **31,** 123-
219   126 (2003).
220 17. Lague, D., Crave, A. & Davy, P. Laboratory experiments simulating the geomorphic response
221   to tectonic uplift. *J. Geophys. Res* **108** (2003) (doi:10.1029/2002JB001893).
222 18. Whipple, K. X. & Tucker, G. E. Dynamics of the stream-power river incision model:
223   Implications for height limits of mountain ranges, landscape response timescales, and
224   research needs. *J. Geophys. Res.* **104,** 17661-17674 (1999).
225 19. Whipple, K. X. Fluvial landscape response time: How plausible is steady-state denudation?
226   *Am. J. Sci.* **301,** 313-325 (2001).
227 20. Leopold, L. B. & Maddock Jr, T. The hydraulic geometry of stream channels and some
228   physiographic implications. U. S. Geol Surv. Prof. Pap. **252** (1953).
229 21. Turowski, J. M., Lague, D., Crave, A. & Davy, P. Experimental channel response to tectonic
230   uplift. *J. Geophys. Res* **111** (2006) (doi:10.1029/2005JF000306).
231 22. Wobus, C. W., Tucker, G. E. & Anderson, R. S. Self-formed bedrock channels. *Geophys. Res.*
232   *Lett.* **33** (2006) (doi:10.1029/2006GL027182).
233 23. Whittaker, A. C., Cowie, P. C., Attal, M., Tucker, G. E. & Roberts, G. P. Bedrock channel
234   adjustment to tectonic forcing: Implications for predicting river incision rates. *Geology* **35,**
235   103-106 (2007).
236 24. Strecker, M. R., Cerveny, P., Bloom, A. L. & Malizia, D. late Cenozoic tectonism and landscape
237   development in the foreland of the Andes: Northern Sierras Pampeanas (26°S-28°S),
238   Argentina. *Tectonics* **8,** 517-534 (1989).
239 25. Strecker, M. R., Alonso, R. N., Bookhagen, B., Carrapa, B., Hilley, G. E., Sobel, E. R. & Trauth,
240   M. H. Tectonics and climate of the Southern Central Andes. *Ann. Rev. Earth Planet. Sci*. **35,**
241   747-787 (2007).
242 26. Bookhagen, B. & Strecker, M. R. Orographic barriers, high-resolution TRMM rainfall, and
243   relief variations along the eastern Andes. *Geophys. Res. Lett.* **35** (2008)
244   (doi:1029/2007GL032011).
245 27. Kleinert, K. & Strecker, M. R. Climate change in response to orographic barrier uplift: Paleosol
246   and stable isotope evidence from the late Neogene Santa Maria basin, northwestern
247   Argentina. *Geol. Soc. Am. Bull.* **113,** 728-742 (2001).
248 28. Sobel, E. R., Hilley, G. E. & Strecker, M. R. Formation of internally drained contractional basins
249   by aridity-limited bedrock incision. *J. Geophys. Res.* **108** (2003) (doi:10.1029/2002JB001883).
250 29. Talling, P. J., Stewart, M. D., Stark, C. P., Gupta, S. & Vincent, S. J. Regular spacing of drainage
251   outlets from linear faults blocks. *Basin Res.* **9,** 275-302 (1997).

252 30. Moyano, M. S. Análisis regional del emplazamiento, sedimentación y evolución sintectónica
253   de los abanicos aluviales cuaternarios de las Sierras Pampeanas Nordoccidentales. Catamarca
254   y Tucumán. Unpublished PhD thesis, Facultad de Ciencias Naturales e IML - Universidad
255   Nacional de Tucumán, 209 p. (2009).
256
257

258 Correspondence and requests for materials should be addressed to S.B.

259

260 **Acknowledgements**

267
268

269 **Figure captions**

270 **Figure 1 Laboratory modelling of landscape dynamics under uniform uplift of the eroded material
271 and lateral precipitation gradient**. The uplift rate is 12 mm h^{-1}. **a**, Evolution of topographic profiles.
272 Each line is the mean elevation along a 20-cm-wide transverse swath calculated from DEMs. The
273 patterns of rainfall forcing are also shown. Note the superimposition of the topographic profiles at
274 the end of the first step, which implies a steady-state between uplift and erosion[16,17]. **b**, Evolution of
275 mean and maximum (drainage divide) elevations of the model. Error bars give the standard deviation
276 of the mean. The solid line indicates the amount of applied uplift, i.e. elevation of the model if no
277 erosion occurred. The line is only interrupted upward for graphical convenience; uplift forcing was
278 applied during the entire experiment at a constant rate. Note that the constancy of mean and
279 maximum elevations during the first evolution step implies a steady-state between uplift and
280 erosion[16,17] and the absence of a steady-state from the application of the rainfall gradient. **c**,
281 Evolution of the normalized divide position[6], highlighting the asymmetry development from the
282 application of the rainfall gradient. **d**, Photographs of three stages of landscape evolution, taken at
283 steady-state (600') and during the subsequent divide migration (940 and 1300'). The model width on
284 the view is 400 mm.

285

286 **Figure 2 Landscape response to main drainage divide (MDD) migration**. The images are successive
287 shaded surface views of the driest side of the model DEMs (views are ~200 X 300 mm) with
288 superposition of drainage networks as extracted from DEMs using a steepest-slope flow routine. The
289 width of individual channels on the images only depends on the pixel size of the DEMs (0.5 mm) and
290 does not reflect the width dependency with discharge or slope. The images illustrate the migration of
291 the MDD, the induced shortening of the drainage basins and the split of their drainage network. The
292 splitting mechanism induced the abandonment of former parts of the landscape where tributaries

293   were initially connected (open arrows) and their subsequent uplift, leading to the development of
294   new hillcrests (solid arrows). This mechanism consequently leads to the individuation of two
295   drainage basins from a single former one.

296

297   **Figure 3 Detailed geomorphic evolution of a drainage basin. a**, Photographs taken from the
298   driest side of the experimental landscape showing the location of the studied drainage basin (orange
299   arrow) and of some selected points of the landscape whose elevation history is detailed. **b**, Time-
300   evolution of mean runoff within the selected drainage basin, water flux at outlet and basin size. **c**,
301   Time-evolution of the longitudinal profile of the main trunk channel. The stack of longitudinal profiles
302   until 600 minutes corresponds to the steady-state between erosion and uplift during the first phase
303   of uniform rainfall. Note the progressive shortening and steepening of the channel once the rainfall
304   gradient is applied and the existence of a temporary steady-state before splitting occurred. **d**,
305   Detailed elevation history of three selected points of the landscape. Point A is located in a channel
306   and it remains in the channel during the entire experiment. After the application of the rainfall
307   gradient, its elevation first increases but rapidly stabilizes during the temporary steady-state; it is
308   finally uplifted after splitting occurred. Point B is located on a permanent hillcrest that separates two
309   main drainage basins. It is continuously uplifted after the application of the rainfall gradient. The
310   evolution of point C is a combination of histories of points A and B. It corresponds to a channel with a
311   similar evolution than A until splitting occurred. It is then uplifted and ends on a hillcrest that divides
312   up a former single drainage basin into two individual ones. Dotted lines show the trend of applied
313   uplift ("rock uplift") and therefore indicate the elevation of points that are passively uplifted, i.e.
314   where no erosion occurred.

315

316   **Figure 4 Model of drainage basin response to drainage divide migration** (see text for comments).
317   Blue colours show active streams, whereas orange colours show hypothetical floodplain deposits.
318   Note that some of these deposits can be passively uplifted and observed on the hillcrest separating
319   two newly-formed drainage basins. These deposits would be classically interpreted as resulting from
320   relief inversion or river capture.

321

322   **Figure 5 Topography and drainage networks of the Sierra Aconquija, northwestern Argentina. a**,
323   Map showing the topography of the Sierra Aconquija, major tectonic elements and mean annual
324   precipitation (dotted blue lines, in mm yr^{-1}; after ref. 10). **b**, Perspective view highlighting the
325   topographic asymmetry of the range. **c**, Images showing examples of drainage networks located on
326   the driest side of the Sierra Aconquija where different stages of drainage splitting likely are
327   represented, following the model shown in Fig. 4 (images from OpenAerialMap.org, except 1&2:
328   GoogleEarth). Examples 1 and 2 are cases where two tributary streams do not connect at valleys'
329   junction, but flow separately within a single valley floor (open arrows). The same configuration is
330   observed in example 3, except that the two parallel-flowing streams are separated by elevated fluvial
331   deposits (solid arrow) whose mapping[30] shows that they constituted a single alluvial body that
332   extended upstream along the two streams. Consequently, it likely represents an example where

333   drainage splitting is associated to the nascent of a new hillcrest. Example 4 shows the case of a

334   hillcrest (solid arrow) separating two drainage basins whose outlets are very close and whose general

335   shapes suggest that they initially formed a single drainage basin. This assumption is reinforced by the

336   abrupt change in the flowpath direction of one river, suggesting a former connection between the

337   two drainage basins (white dotted line), and by the existence of a system of alluvial fans whose size

338   suggests feeding by a basin larger than the two present ones. This last example would thus represent

339   the ultimate case of the splitting mechanism.

340

341   **Supplementary Figure. Spacing of drainage basin outlets of experimental landscapes plotted**

342   **against drainage basin lengths.** The linear relationship shown here is similar to the trend observed in

343   natural landscapes[9]. The linear fit defines a spacing ratio (ratio between the spacing and the length[9])

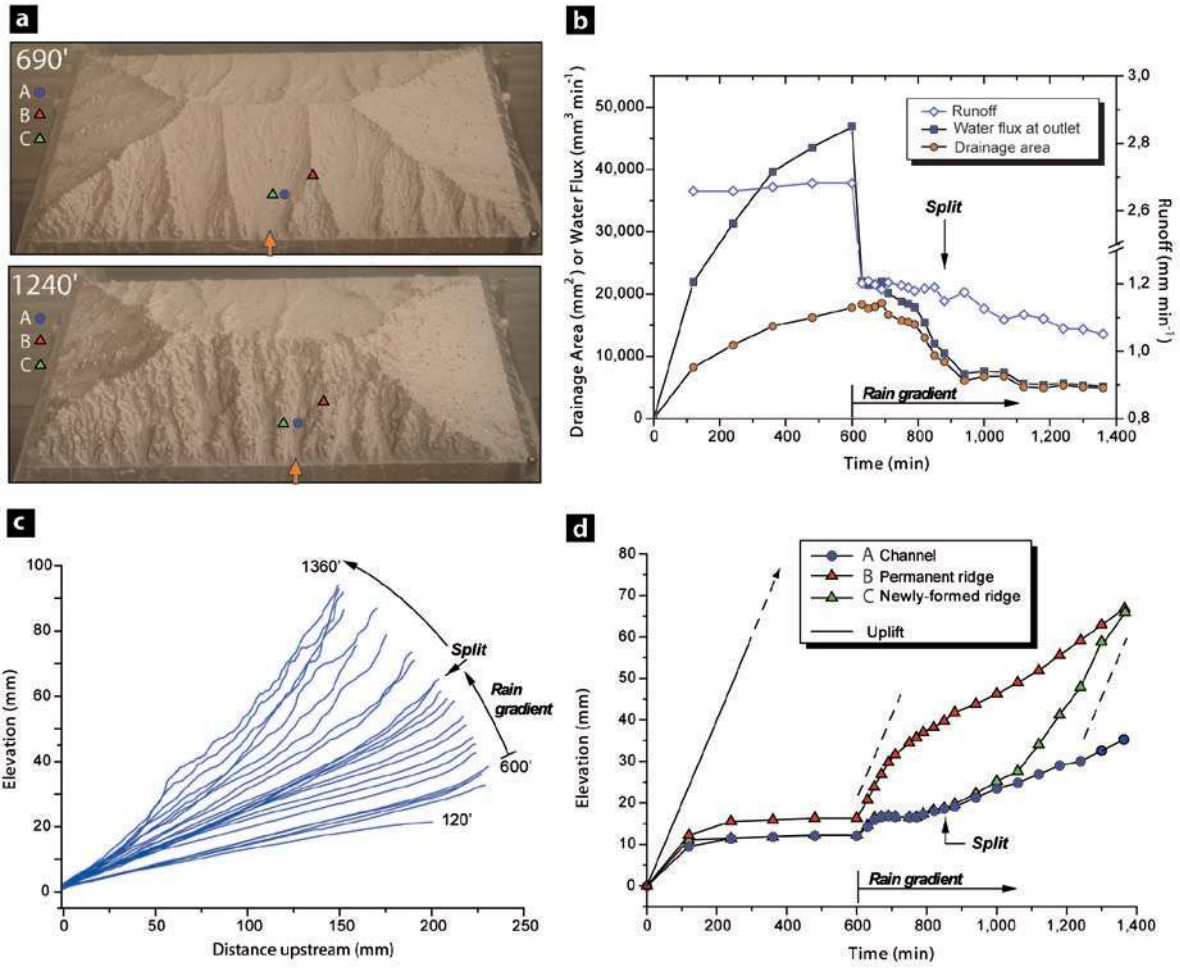344   of 2.22, whereas the values range between 1.91 and 2.23 in natural landscapes[9].
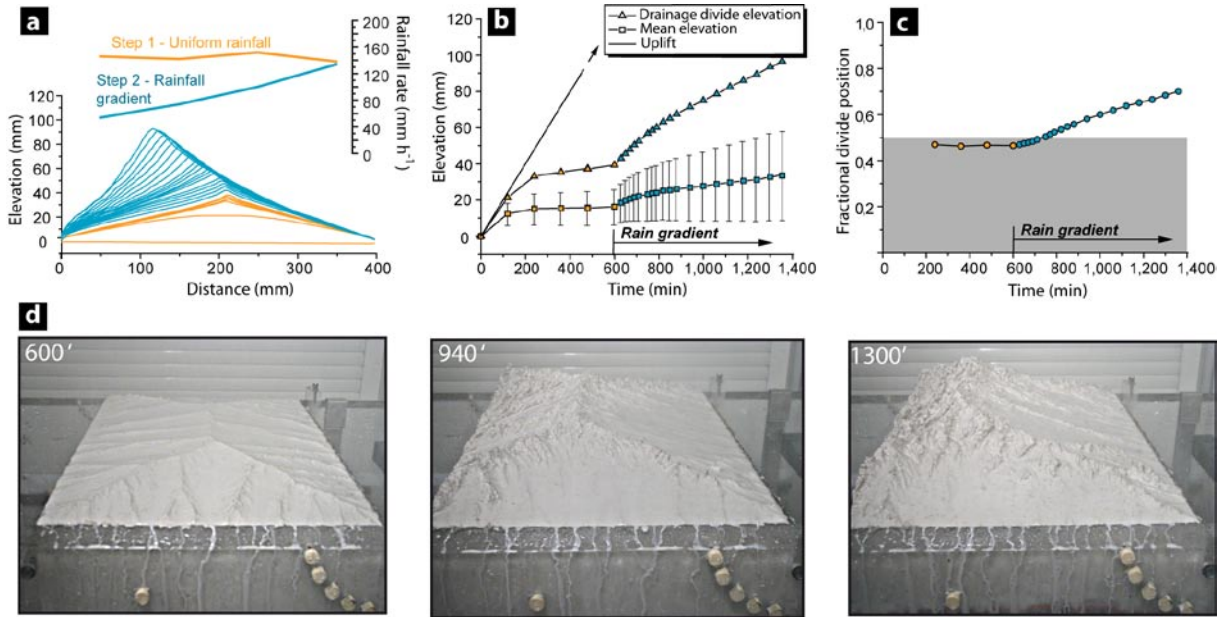
NGS-2009-06-00693
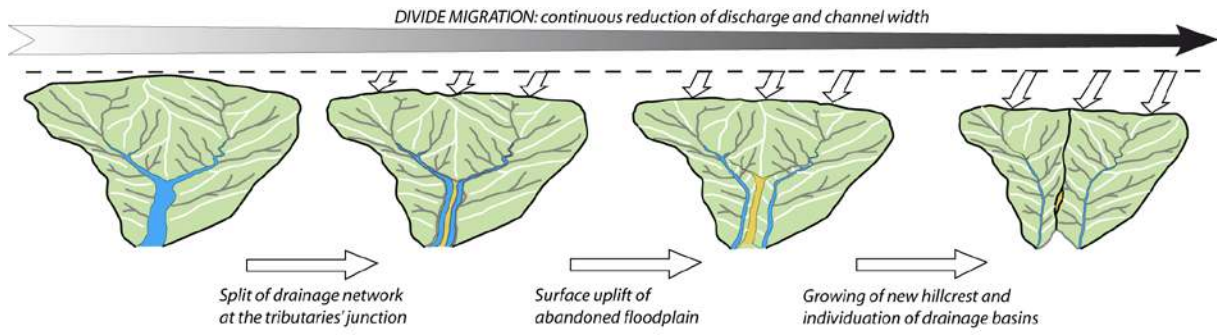BONNET Figure 1
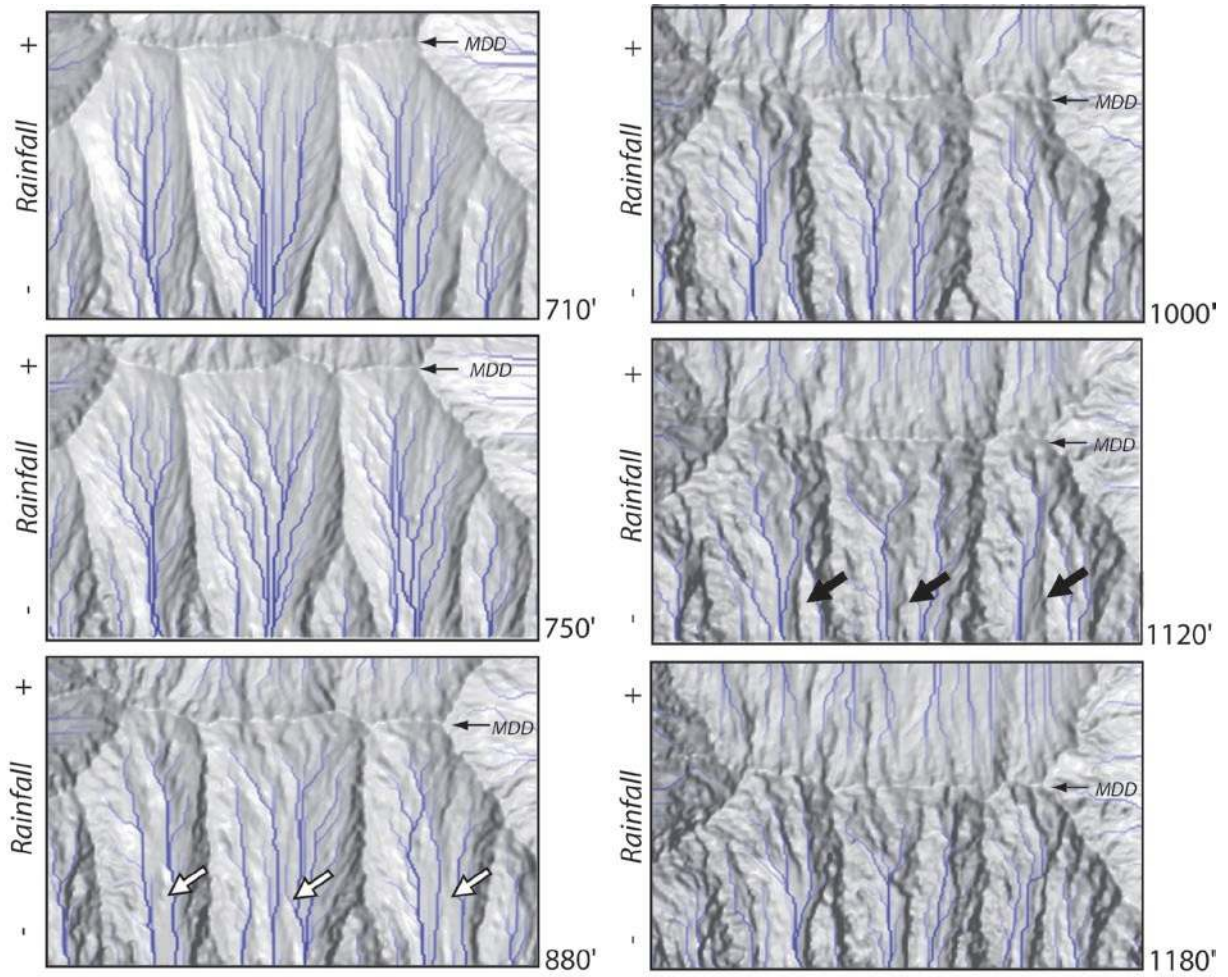
NGS-2009-06-00693
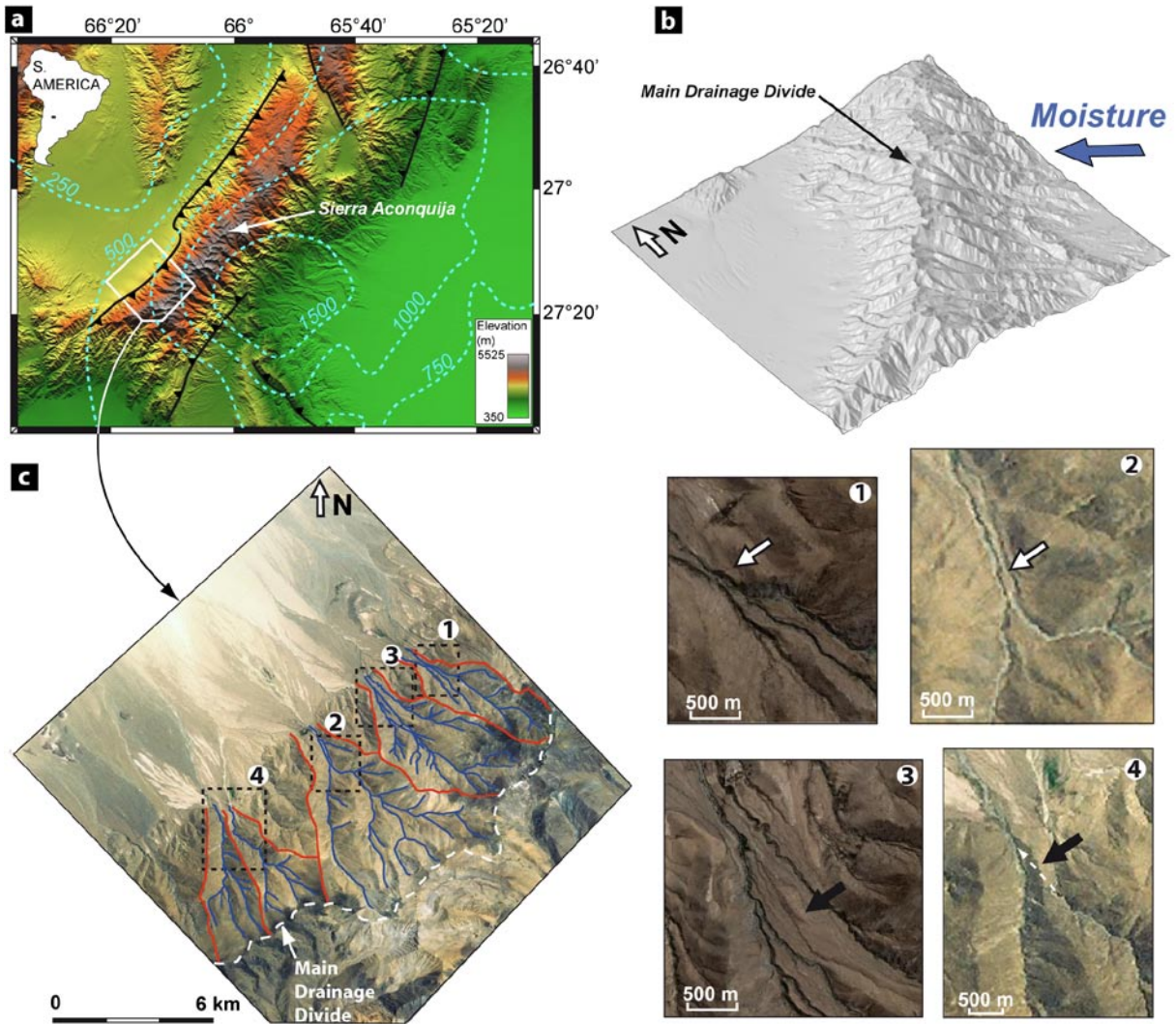BONNET Figure 2

346

NGS-2009-06-00693
BONNET Figure 3

349

NGS-2009-06-00693
BONNET Figure 4

350

NGS-2009-06-00693
BONNET Figure 5